GAS-PHASE CLUSTERING OF NO^+ WITH H_2S AND H_2O

Milan UHLÁR[a] and Ivan ČERNUŠÁK[b,*]

[a] *Institute of Physics, Faculty of Art and Science, Silesian University, Bezručovo nám. 13, CZ-746 01 Opava 1, Czech Republic; e-mail: milan.uhlar@fpf.slu.cz*

[b] *Department of Physical and Theoretical Chemistry, Faculty of Natural Sciences, Comenius University, SK-84215 Bratislava, Slovakia; e-mail: cernusak@fns.uniba.sk*

Received May 18, 2007
Accepted July 13, 2007

Dedicated to Professor Štefan Toma on the occasion of his 70th birthday.

The complex $NO^+ \cdot H_2S$, which is assumed to be an intermediate in acid rain formation, exhibits thermodynamic stability of $\Delta H°_{300} = -76$ kJ mol^{-1}, or $\Delta G°_{300} = -47$ kJ mol^{-1}. Its further transformation via H-transfer is associated with rather high barriers. One of the conceivable routes to lower the energy of the transition state is the action of additional solvent molecule(s) that can mediate proton transfer. We have studied several $NO^+ \cdot H_2S$ structures with one or two additional water molecule(s) and have found stable structures (local minima), intermediates and saddle points for the three-body $NO^+ \cdot H_2S \cdot H_2O$ and four-body $NO^+ \cdot H_2S \cdot (H_2O)_2$ clusters. The hydrogen bonds network in the four-body cluster plays a crucial role in its conversion to thionitrous acid.

Keywords: Hydrogen bond; Hydration; Nitric oxide cation; Hydrogen sulfide; Quantum chemistry.

The formation of ion clusters and ion-molecule complexes plays an important role in many branches of physics, chemistry and biology because these processes are relevant to gas-phase solvation, acid-base equilibria, combustion, catalysis and atmospheric phenomena. They often include various types of intermolecular interactions which can become the initial step of chemical reaction. Of particular interest among them are those ion-molecule interactions that are part of important gas-phase solvation processes in the stratosphere (altitudes 15–50 km) and ionosphere (altitudes above 50 km).

Quite a few studies of ion-molecule reactions have been focused on the clustering phenomena related to nitrogen oxides which may exist in the upper Earth atmosphere[1–6]. Nitrogen oxides enter into an important part of the atmospheric chemical reactivity[7]. From the environmental point of

doi:10.1135/cccc20071122

view, the most abundant are N_2O, NO and NO_2, collectively denoted as the N_xO_y family. They are produced by photochemical processes (from molecular nitrogen and oxygen) during lightning and due to anthropogenic activity.

Nitric oxide is the parent molecule for the ionic species NO^+. The nitric oxide cation is one of the major ionic constituents of the ionosphere in the D- (altitudes 50–90 km), E- (altitudes 90–140 km) and F-layers (above 140 km)[8]. In the D-layer, also ion O_2^+ and traces of Mg^+, Fe^+, Na^+, K^+ and Cs^+ were observed. NO^+ has an impact on both ion-molecule chemistry and physics of the atmosphere since it is quite abundant and can influence not only numerous chemical processes but also physical properties of the atmosphere, such as electric conductivity. Concentration of this ion in higher layers of the ionosphere, E and F, is lower due to recombination with free electrons[9]. NO^+ is produced[7] either directly by day-time photo-ionization of nitric oxide by solar Lyman-α radiation (λ ~120 nm)

$$NO_2 + h\nu \rightarrow NO + O$$

$$NO + h\nu \rightarrow NO^+ + e$$

or indirectly, from N_2 and O_2 ionized by X-rays:

$$O^+ (^4S) + N_2 (X^1\Sigma_g^+) \rightarrow NO^+ (X^1\Sigma^+) + N (^4S)$$

$$N_2^+ (A^2\Pi) + NO (X^2\Pi) \rightarrow N_2 (X^1\Sigma_g^+) + NO^+ (X^1\Sigma^+) .$$

Molecular ions present in the D-region can react with water vapour to produce water cluster ions, gravitationally penetrate through the border between ionosphere and stratosphere and participate in clustering reactions with other atmospheric molecules originating from natural or industrial sources[9]. The key step in these processes, atmospheric clustering of NO^+ with water, received considerable attention in the last three decades, as reflected by numerous experimental and theoretical studies and reviews[8–20].

The $NO^+ \cdot H_2O$ ion-molecule complex has been suggested as a key intermediate in the production of various hydronium-water complexes, but the efficient formation of this particular complex in the atmosphere is believed to depend strongly on the presence and abundance of the related complexes $NO^+ \cdot X$ (where X is O_2, N_2, CO_2). The atmospheric conversion process can include as the first step the formation of a complex between NO^+ and molecule X, followed by rapid exchange reaction. For example, for X = CO_2

Dunkin et al.[21] have proposed the sequence with the participation of a third particle

$$NO^+ + CO_2 + M \rightarrow NO^+ \cdot CO_2 + M$$

$$NO^+ \cdot CO_2 + H_2O \rightarrow NO^+ \cdot H_2O + CO_2 \ .$$

The importance of NO^+ in atmospheric chemistry can be illustrated by its relation to $H^+ \cdot (H_2O)_n$ clusters. Water cluster ions $H^+ \cdot H_2O$ and $H^+ \cdot (H_2O)_2$ have been found to dominate the D-region around the altitude 80 km and can affect both clustering and exchange reactions of NO^+ with a variety of neutral ligands (N_2, CO_2). On the basis of the flowing-afterglow experiments performed by Fehsenfeld and Fergusson[10,21] as well as by Lineberger and Puckett[22], it was suggested that the formation of cluster ions $H^+ \cdot (H_2O)_n$ can proceed from $NO^+ \cdot H_2O$ in a multistep hydration[10,22,23] mechanism

$$NO^+ \cdot H_2O + H_2O \rightarrow NO^+ \cdot (H_2O)_2$$

$$NO^+ \cdot (H_2O)_2 + H_2O \rightarrow NO^+ \cdot (H_2O)_3$$

$$NO^+ \cdot (H_2O)_3 + H_2O \rightarrow HONO + H^+ \cdot (H_2O)_3 \ .$$

$H^+ \cdot (H_2O)_n$ clusters with even higher n imply the production of HNO_3 in the upper atmosphere[10]. Thus, NO^+ is indirectly participating in acid rain formation. These findings were confirmed by pulsed high-pressure ion source mass spectroscopy[24] and vibrational predissociation laser spectroscopy supported by ab initio calculations[19].

Less is known about the interactions of NO^+ with the other conceivable neutral ligands which can be present at the border between stratosphere and ionosphere as a consequence of industrial production or volcanic activity. Among them, CH_3CN, NH_3, CH_4, CH_3OH, HCN, SO_2, HSO_3 (refs[13,14,25]) were mentioned in the literature. These molecules can collide with NO^+ and form transient structures that, in principle, can either affect NO^+ clustering and subsequent ion-molecule chemistry or can form aerosols. Arijs has stressed the importance of the knowledge of stratospheric ion composition and ion-molecule interactions because it can lead to the detection of trace gases so far unknown[14]. One example of such complexes can be $NO^+ \cdot H_2S$. In regions with strong air pollution or increased volcanic activity hydrogen sulfide or other gases can persist at elevated partial pressure and contribute to NO^+ clustering. A key issue related to the clustering of the $NO^+ \cdot H_2S$ complex with water molecules is the problem of the proton trans-

fer under "wet" conditions leading to thionitrous acid[26] (HSNO). Recently, we have published a pilot study of the potential energy surface of this complex using ab initio methods investigating thermodynamic stability of various isomers of $NO^+ \cdot H_2S$ and the structural features of their model harmonic IR spectra[27]. Our calculations implied no proton transfer in the $NO^+ \cdot H_2S$ system under dry conditions because of unacceptably high energy barriers associated with this process.

One of the conceivable routes to lower the energy of the transition state is the assistance of additional solvent molecule(s) which can mediate the proton transfer. The aim of this paper is to investigate the possibility of the conversion of water-clustered $NO^+ \cdot H_2S$ into HSNO via proton-transfer reaction and the role of water molecules in this mechanism.

METHODS

In this study, we have limited our investigations of NO^+ clustering to two types of complexes: the three-body cluster $NO^+ \cdot H_2S \cdot H_2O$ and the four-body cluster $NO^+ \cdot H_2S \cdot (H_2O)_2$. For the geometry optimizations of the three-body cluster we have used DFT-BLYP [28], DFT-B3LYP [29] and MP2 [30] methods with correlation-consistent basis set of triple-zeta quality[31] (cc-pVTZ), while only the MP2/cc-pVTZ method was used for the four-body cluster. For the three-body cluster we have selected the BLYP and B3LYP functionals to check their performance against the MP2 method because we plan to use DFT for modelling of larger clusters. Harmonic frequencies of each structure were calculated to confirm the nature of the stationary point. For both types of complexes we have also evaluated single-point energies at the CCSD(T) level[30,32,33] using cc-pVTZ basis set at MP2/cc-pVTZ optimal geometries to obtain final reaction profiles. For the CCSD(T) energy profile (ΔH and ΔG values) we have used MP2 frequencies in thermochemistry calculations.

We have also checked the basis set superposition error (BSSE) for the cc-pVTZ basis set for the cases where the geometry changes accompanying the cluster formation were negligible. This was possible in evaluating the interaction energy of three models: $NO^+ \cdot H_2S + H_2O$, $NO^+ \cdot H_2O + H_2S$ and $NO^+ \cdot H_2S \cdot H_2O + H_2O$ at the CCSD(T) level. The counterpoise correction[34] (CPC) was applied in the calculations of interaction energies for the resulting clusters. Thermodynamic properties, reaction enthalpies and Gibbs energies, were calculated assuming the ideal gas and rigid-rotor/harmonic oscillator approximation. All calculations were carried out using the Gaussian 03 [35] and ACES-II [36] suites of programs. Ball-and-stick structures were produced using MOLDEN [37].

RESULTS AND DISCUSSION

The optimized structures for monohydrated $NO^+ \cdot H_2S$ are depicted in Figs 1–3. To illustrate the performance of the BLYP, B3LYP and MP2 methods we have shown the values of bond lengths (from top to bottom for each row) in Figs 1–3. For the remaining structures we present only MP2/cc-pVTZ geometry parameters. Reaction profiles for the $NO^+ \cdot H_2S \cdot H_2O$ clus-

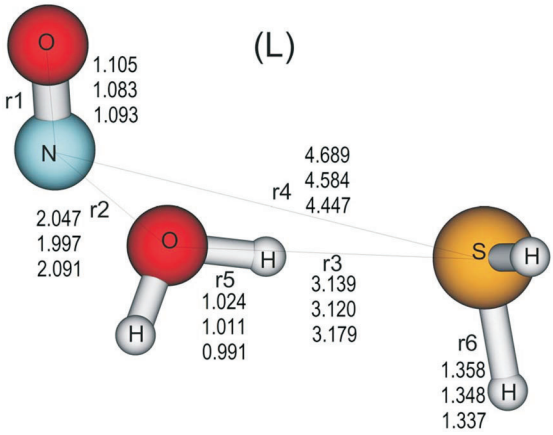

FIG. 1
Local minimum $NO^+ \cdot H_2O \cdot H_2S$ (L)

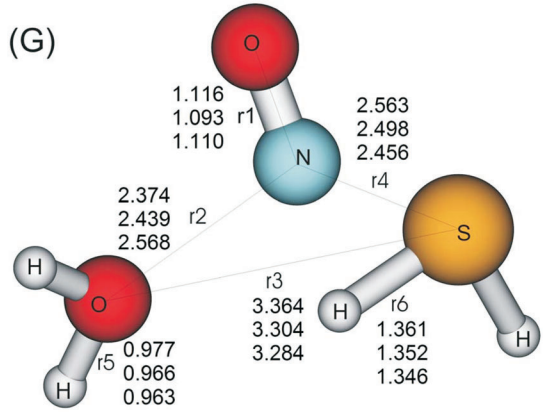

FIG. 2
Global minimum $NO^+ \cdot H_2S \cdot H_2O$ (G)

ter are in Figs 4 (ΔH_{298}) and 5 (ΔG_{298}). The optimized structures for bihydrated $NO^+ \cdot H_2S$ are depicted in Figs 6–11. Reaction profiles for the $(H_2O)_2 \cdot NO^+ \cdot H_2S$ clusters are depicted in Fig. 12. The MP2/cc-pVTZ Cartesian coordinates of the reactants, products, intermediates and transition states considered in this study are given in Supplementary material.

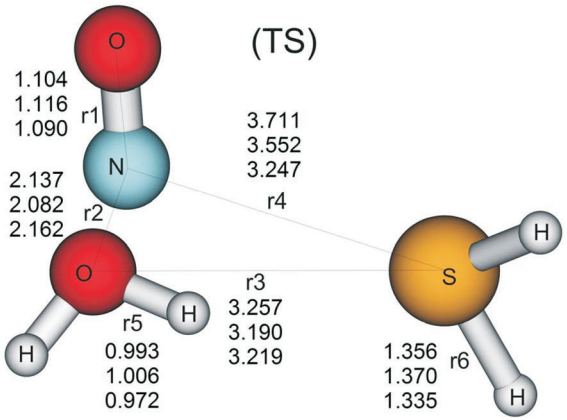

FIG. 3
Transition state between (L) and (G)

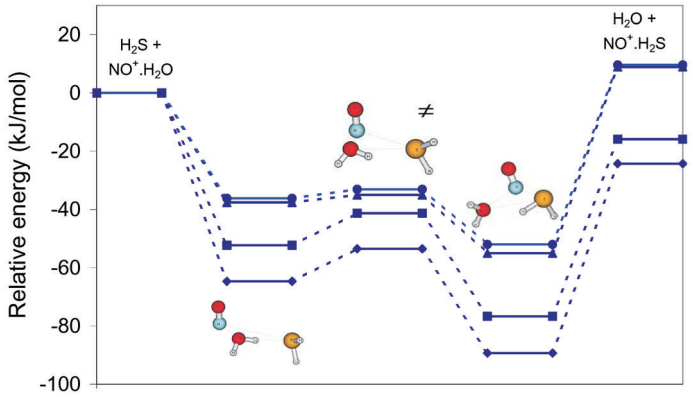

FIG. 4
Enthalpy profiles for the cluster $H_2O \cdot NO^+ \cdot H_2S$: ◆ BLYP, ■ B3LYP, ▲ MP2, ● CCSD(T)

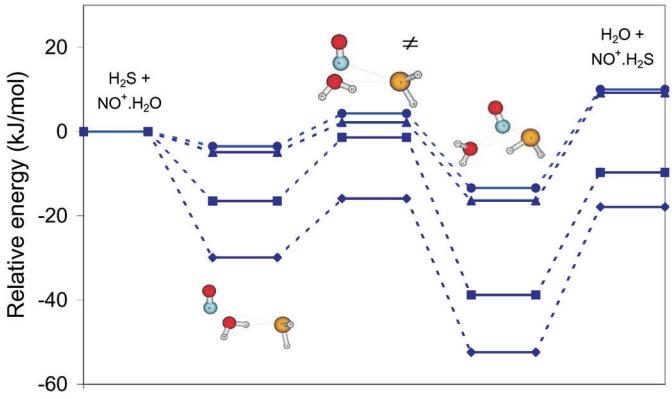

FIG. 5
Gibss energy profiles for the cluster $H_2O{\cdot}NO^+{\cdot}H_2S$: ◆ BLYP, ■ B3LYP, ▲ MP2, ● CCSD(T)

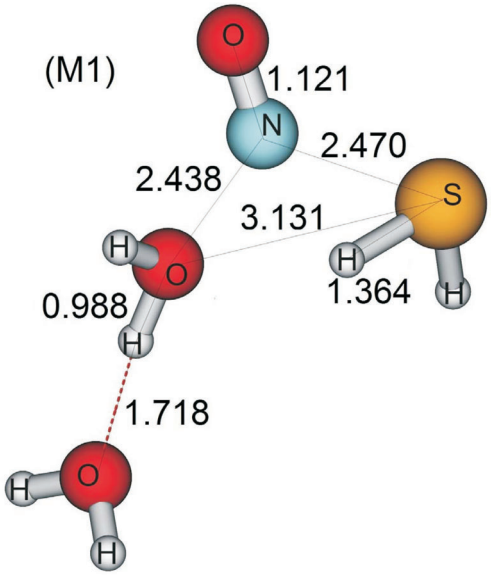

FIG. 6
Minimum $(H_2O)_2{\cdot}NO^+{\cdot}H_2S$ (M1)

$NO^+ \cdot H_2S \cdot H_2O$

We have found three stationary points on the $NO^+ \cdot H_2S \cdot H_2O$ potential energy surface: local minimum, global minimum and transition state. The local minimum corresponds to the sequential structure $NO^+ \cdot H_2O \cdot H_2S$ (Fig. 1) that can be regarded as a complex $NO^+ \cdot H_2O$ solvated by a H_2S molecule. In

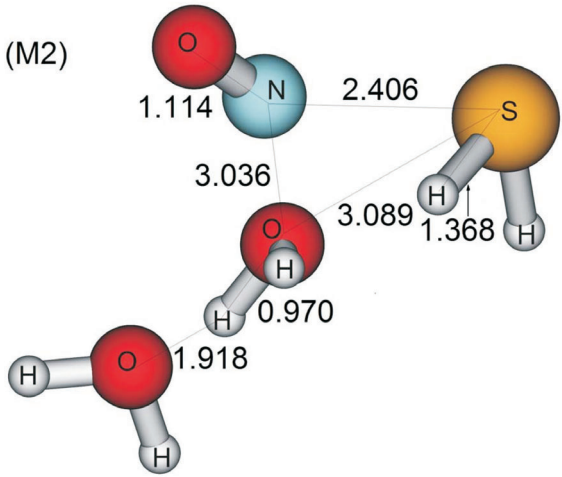

FIG. 7
Minimum $(H_2O)_2 \cdot NO^+ \cdot H_2S$ (M2)

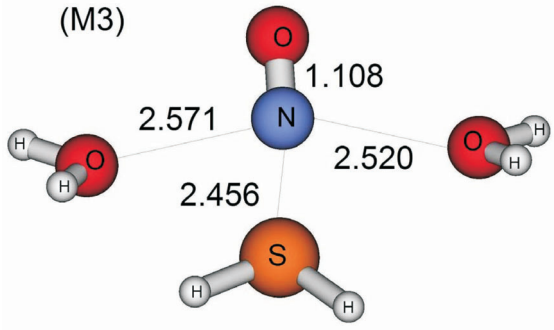

FIG. 8
Quasi-symmetrical minimum $H_2O \cdot NO^+ \cdot H_2S \cdot H_2O$ (M3)

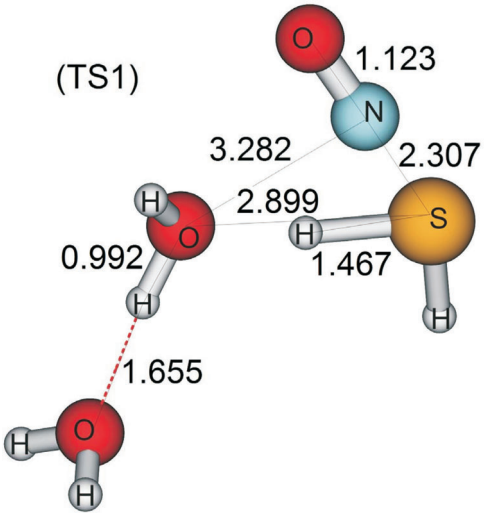

FIG. 9
Transition state 1 for the proton transfer (TS1)

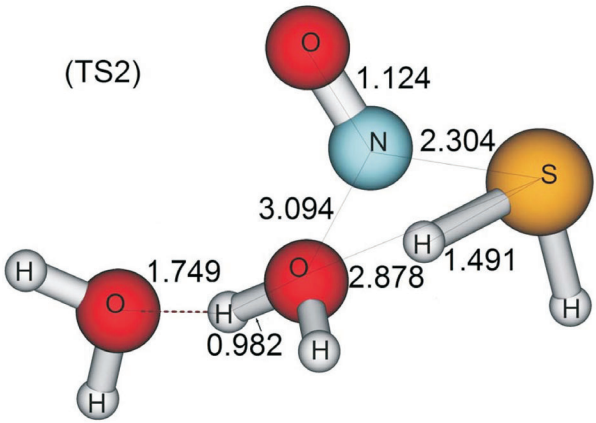

FIG. 10
Transition state 2 for the proton transfer (TS2)

the global minimum (Fig. 2) the roles of ligands are reversed and the structure can be regarded as a distorted three-membered ring in which the complex $NO^+ \cdot H_2S$ is solvated by a water molecule. The conversion from local to global minimum is associated with the transition state, $[NO^+H_4SO]^{\neq}$ (Fig. 3).

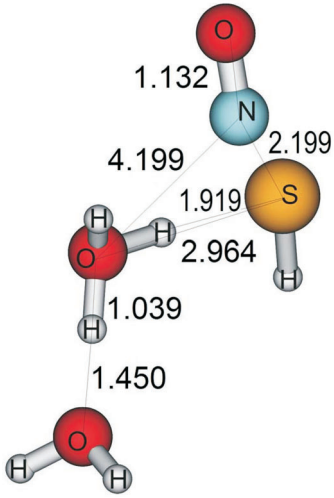

FIG. 11
Intermediate $H_2O \cdot H_3O^+ \cdot HSNO$

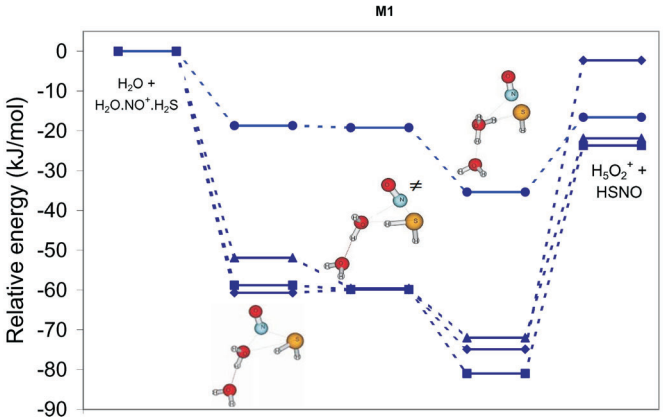

FIG. 12
Reaction profiles for the cluster $(H_2O)_2 \cdot NO^+ \cdot H_2S$ (M1): ◆ ΔE MP2, ■ ΔE CCSD(T), ▲ ΔH_{298}, ● ΔG_{298}

The trajectory from the transition state to both minima was checked by the IRC procedure at the MP2/cc-pVTZ level. Although the agreement between BLYP, B3LYP and MP2 geometries is only qualitative, all three methods provide comparable structures associated with the isomerization path between local and global minimum. All attempts to locate the other stationary points eventually leading to proton transfer from H_2S to H_2O in this complex failed. This is in accord with previous studies which did not indicate proton transfer for any monosolvated species $NO^+ \cdot X$ [23].

We may consider five processes associated with the $NO^+ \cdot H_2S \cdot H_2O$ complex:

$$NO^+ \cdot H_2S + H_2O \rightarrow NO^+ \cdot H_2S \cdot H_2O \quad (G) \qquad (1)$$

$$NO^+ \cdot H_2O + H_2S \rightarrow NO^+ \cdot H_2O \cdot H_2S \quad (L) \qquad (2)$$

$$NO^+ \cdot H_2S \cdot H_2O \rightarrow NO^+ \cdot H_2O \cdot H_2S \qquad (3)$$

$$NO^+ \cdot H_2S \cdot H_2O \rightarrow [NO^+H_4SO]^{\neq} \quad (TS)\,. \qquad (4)$$

The first two refer to the formation of three-body complexes, the process (*1*) leads to the global minimum (denoted as G) while the process (*2*) leads to the local one (denoted as L). Conversion from the global to the local minimum can be accomplished via the transition state (TS, processes (*3*) and (*4*)). Energy quantities associated with the processes (*1*)–(*4*) are in Table I. The BSSE for (*1*) and (*2*) are small and amount to 3 and 6 kJ mol^{-1}, respectively. There is a significant entropy contribution in the association reactions (*1*) and (*2*) resulting in significantly lower complexation Gibbs energies than enthalpies, especially for the local minima (see also Figs 4 and 5). For the association reactions (*1*) and (*2*) both BLYP and B3LYP overestimate the enthalpy and Gibbs energy, compared with MP2 and CCSD(T) results. This means that not only electronic energies are overestimated by both DFT approaches but also the respective quantities entering the partition functions (frequencies, equilibrium geometries) differ significantly from MP2 data. This is clearly visible in Figs 4 and 5, energy profiles for MP2 and CCSD(T) are shallow compared with DFT approaches. The agreement between DFT approaches and MP2 or CCSD(T) is better for isomerizations ((*3*) and (*4*)), where favourable cancellation of errors takes place. Thus, for the future studies of dynamics and/or isomerizations in similar or

larger clusters, one can expect plausible results also from the BLYP or B3LYP levels of theory. Both temperatures (298 and 250 K) refer to the peak thermochemistry values between day and night. Hence, our results indicate that the potential accumulation of these complexes in the atmosphere most probably takes place during the night.

$(H_2O)_2 \cdot NO^+ \cdot H_2S$

Attaching an additional water molecule to the global minimum G leads to a four-body cluster and has a dramatic effect on its chemistry, compared with the three-body cluster. The energy gain accompanying the association of the second water molecule (processes (*5*) and (*10*)) is only slightly smaller than pertinent ΔH or ΔG for the three-body cluster, reflecting strong coop-

TABLE I
Energy profile (in kJ mol^{-1}) for the $NO^+ \cdot H_2S \cdot H_2O$ complex

Reaction	Energy	(*1*)[a]	(*2*)[b]	(*3*)	(*4*)
BLYP	ΔH_{298}	–65.0	–64.7	24.6	35.8
	ΔG_{298}	–34.5	–29.9	22.5	36.5
	ΔH_{250}	–66.8	–65.1	24.8	36.2
	ΔG_{250}	–39.7	–35.5	22.9	36.4
B3LYP	ΔH_{298}	–60.8	–52.3	24.4	35.4
	ΔG_{298}	–29.1	–16.5	22.3	37.4
	ΔH_{250}	–61.7	–52.6	25.0	35.9
	ΔG_{250}	–34.3	–22.3	22.6	37.2
MP2	ΔH_{298}	–63.9	–37.6	17.4	20.0
	ΔG_{298}	–25.6	–4.9	11.5	18.6
	ΔH_{250}	–64.3	–37.8	17.5	20.2
	ΔG_{250}	–31.8	–10.2	12.4	19.0
CCSD(T)	ΔH_{298}	–61.6	–36.2	15.8	18.9
	ΔG_{298}	–23.4	–3.5	9.9	17.7
	ΔH_{250}	–62.1	–36.4	16.0	19.2
	ΔG_{250}	–29.6	–8.8	10.8	17.9

[a] $\Delta E_{CCSD(T)}$ = –68.0 kJ mol^{-1}, $\Delta E_{CCSD(T)+CPC}$ = –61.6 kJ mol^{-1}. [b] $\Delta E_{CCSD(T)}$ = –41.6 kJ mol^{-1}, $\Delta E_{CCSD(T)+CPC}$ = –38.6 kJ mol^{-1}.

eration effects in the formation of the four-body cluster. The BSSE for (*5*) is small (3 kJ mol^{-1}), we could not evaluate BSSE for process (*10*) because its calculation is obscured by a large geometry deformation in the resulting cluster (compared with subsystems) and thus not well defined. The three minima found on this potential energy surface are in Figs 6–8. Two of them (Figs 6 and 7) are complexes containing hydrogen bonded-network $H_2O\cdots H_2O$ in which the additional water molecule acts as a proton acceptor. The first complex, $(H_2O)_2\cdot NO^+\cdot H_2S$ (denoted M1), is associated with the crossing of the transition state (Fig. 9) and its transformation to the intermediate $H_2O\cdot H_3O^+\cdot HSNO$ (Fig. 11) and leading to hydrated hydroxonium cation and thionitrous acid:

$$H_2O + H_2O\cdot NO^+\cdot H_2S \rightarrow (H_2O)_2\cdot NO^+\cdot H_2S \quad (M1) \qquad (5)$$

$$(H_2O)_2\cdot NO^+\cdot H_2S \rightarrow TS1 \qquad (6)$$

$$H_2O\cdot H_3O^+\cdot HSNO \rightarrow TS1 \qquad (7)$$

$$(H_2O)_2\cdot NO^+\cdot H_2S \rightarrow H_2O\cdot H_3O^+\cdot HSNO \qquad (8)$$

$$H_2O\cdot H_3O^+\cdot HSNO \rightarrow H_5O_2^+ + HSNO\ . \qquad (9)$$

The second complex (M2, Fig. 7) is only slightly higher in energy than M1, the differences in ΔH or ΔG (see columns 2 in Tables II and III) not exceeding 4 kJ mol^{-1}. Both electronic states (M1 and M2) are probably nearly degenerate. The complex M2 is associated with the analogous series of reactions:

$$H_2O + H_2O\cdot NO^+\cdot H_2S \rightarrow (H_2O)_2\cdot NO^+\cdot H_2S \quad (M2) \qquad (10)$$

$$(H_2O)_2\cdot NO^+\cdot H_2S \rightarrow TS2 \qquad (11)$$

$$H_2O\cdot H_3O^+\cdot HSNO \rightarrow TS2 \qquad (12)$$

$$(H_2O)_2\cdot NO^+\cdot H_2S \rightarrow H_2O\cdot H_3O^+\cdot HSNO\ . \qquad (13)$$

The bent hydrogen bond $H_2O\cdots HOH$ present in both minima is the crucial point in the transformation of the $(H_2O)_2\cdot NO^+\cdot H_2S$ isomers because this hydrogen bond is the driving force for the rearrangement of the protons in the $H_2O\cdots H_2O\cdots H_2S$ thread. The water molecule in the centre of the cluster promotes further proton transfer from H_2S to the water dimer (processes of forming TS1 or TS2). The elongation of the pertinent HS-bond from equilibrium position ~1.36/1.37 Å (M1/M2, Figs 6 and 7) to ~1.47/1.49 Å (TS1/TS2,

TABLE II
Energy profile (in kJ mol^{-1}) for the complex $(H_2O)_2\cdot NO^+\cdot H_2S$ (M1). Thermodynamic quantities are based on CCSD(T) energies

Energy quantity	(*5*)	(*6*)	(*7*)	(*8*)	(*9*)
MP2	–60.7	0.8	15.0	–14.2	72.6
CCSD	–54.4	6.5	20.4	–13.8	45.9
CCSD(T)[a]	–58.8	–1.1	21.1	–22.2	57.3
ΔH_{298}	–51.9	–7.7	12.5	–20.1	50.1
ΔG_{298}	–18.7	–0.5	16.2	–16.7	18.8
ΔH_{250}	–52.0	–6.9	12.6	–19.5	50.7
ΔG_{250}	–24.0	–1.6	15.6	–17.2	23.9

[a] $\Delta E_{CCSD(T)+CPC}$ = –55.7 kJ mol^{-1} for process (*5*).

TABLE III
Energy profile (in kJ mol^{-1}) for the complex $(H_2O)_2\cdot NO^+\cdot H_2S$ (M2). Thermodynamic quantities are based on CCSD(T) energies

Energy quantity	(*10*)	(*11*)	(*12*)	(*13*)
MP2	–59.8	2.3	17.4	–15.1
CCSD	–52.4	6.9	22.8	–15.9
CCSD(T)	–57.9	–0.2	22.9	–23.1
ΔH_{298}	–51.2	–6.5	14.3	–20.8
ΔG_{298}	–14.2	–3.1	18.1	–21.2
ΔH_{250}	–51.4	–5.8	14.4	–20.1
ΔG_{250}	–20.1	–3.9	17.5	–21.1

Figs 9 and 10) can be followed. The activation processes (*6*) and (*11*) (Tables II and III) are accompanied by negligible energy changes (the ΔH or ΔG estimates are even negative) but this is the effect of ZPV and thermal corrections. Energy profiles in Fig. 12 offer an alternative picture of the conversion of the cluster from the minimum structure M1 into hydrated intermediate $H_2O{\cdot}H_3O^+{\cdot}HSNO$. The negative CCSD(T) barrier is most probably a geometry effect, since this is a result of single-point calculation at the MP2 geometry. The reverse processes (*7*) and (*12*) are associated with larger barriers indicating slower recombination rates once the intermediate $H_2O{\cdot}H_3O^+{\cdot}HSNO$ has been formed. Again, one can observe large entropy effect. Thus, the structures M1 and M2 are reactive species which are the potential source of hydrated HSNO in the atmosphere.

The third complex (M3, Fig. 8) can be regarded as an association product of the global minimum of the three-body cluster with a second water molecule. Our calculations indicate that its formation is accompanied by similar energy changes as the formation of M1 and M2, e.g., $\Delta H_{298} = -52.6$ kJ mol^{-1} and $\Delta G_{298} = -23.6$ kJ mol^{-1} (based on CCSD(T) energies). This cluster represents a quasi-symmetrical structure that is not reactive, i.e., it does not provide any mechanism for the rearrangement of protons because of the unfavourable $H_2O{\cdots}H_2S{\cdots}H_2O$ network (see Fig. 8) which represents merely electrostatic coordination of the ligands around the NO^+ cation. However, further hydration of this cluster may lead to a similar hydrogen-bonded network and promotion of proton transfer leading to thionitrous acid. Work is in progress along these lines in our laboratory.

CONCLUSIONS

We have shown that nitrosonium cation can form stable but relatively weakly-bound complexes with hydrogen sulfide and water under both laboratory and atmospheric conditions. The binding energy is of the order of a medium-strength hydrogen bond. Gradual addition of water molecules changes dramatically the chemistry of clusters. The calculations indicate that the three-body clusters, $NO^+{\cdot}H_2S{\cdot}H_2O$ or $NO^+{\cdot}H_2O{\cdot}H_2S$ once formed, do not undergo further changes and may serve merely as a reservoir for subsequent formation of higher clusters. On the other hand, the four-body cluster, possessing a favorable hydrogen bond, may easily be converted to the thionitrous acid. Our model calculations indicate that the transformation of the four-body cluster depends on the approach of a second water molecule. Therefore, for better understanding of NO^+ clustering and related chemistry, it is desirable to study also the dynamics of these clusters scan-

ning a larger number of possible trajectories at temperatures mimicking the conditions of the upper atmosphere.

This project was supported by the Slovak Research and Development Agency (grant No. APVV-20-018405) and by the Slovak Grant Agency VEGA (grant No. 1/3560/06). We thank the Ministry of Education, Youth and Sports of the Czech Republic (research project MSM 4781305903) for computational support.

REFERENCES

1. Wincel H.: *Chem. Phys. Lett.* **1998**, *292*, 193.
2. Wincel H., Mereand E., Castleman J. A. W.: *J. Phys. Chem.* **1994**, *98*, 8606.
3. Wincel H.: *Int. J. Mass Spectrom.* **2003**, *226*, 341.
4. Wincel H.: *Int. J. Mass Spectrom.* **2000**, *203*, 93.
5. Hiraoka K., Fujimaki S., Aruga K., Yamabe S.: *J. Phys. Chem.* **1994**, *98*, 8295.
6. Hiraoka K., Yamabe S.: *J. Chem. Phys.* **1991**, *95*, 6800.
7. Manahan S. E.: *Environmental Chemistry*. CRC Press LLC, Boca Raton 1999.
8. Ye L., Cheng H.-P.: *J. Chem. Phys.* **1998**, *108*, 2015.
9. Viggiano A. A.: *Phys. Chem. Chem. Phys.* **2006**, *8*, 2557.
10. Fehsenfeld F. C., Ferguson E. E.: *J. Geophys. Res., [Space Phys.]* **1969**, *74*, 2217.
11. Thomas L.: *Ann. Geophys.* **1983**, *1*, 61.
12. Keese R. G., Castleman J. A. W.: *Ann. Geophys.* **1983**, *1*, 75.
13. Arijs E.: *Ann. Geophys.* **1983**, *1*, 149.
14. Arijs E.: *Planet. Space Sci.* **1992**, *40*, 255.
15. Firanescu G., Hermsdorf D., Ueberschaer R., Signorell R.: *Phys. Chem. Chem. Phys.* **2006**, *8*, 4149.
16. Hammam E., Lee E. P. F., Dyke J. M.: *J. Phys. Chem. A* **2000**, *104*, 4571.
17. Hammam E., Lee E. P. F., Dyke J. M.: *J. Phys. Chem. A* **2001**, *105*, 5528.
18. Lee E. P. F., Dyke J. M.: *Mol. Phys.* **1991**, *73*, 375.
19. Choi J.-H., Kuwata K. T., Haas B.-M., Cao Y., Johnson M. S., Okumura M.: *J. Chem. Phys.* **1994**, *100*, 7153.
20. Mack P.: *Chem. Phys.* **1997**, *218*, 243.
21. Dunkin D. B., Fehsenfeld F. C., Schmeltekopf E. E., Ferguson E. E.: *J. Chem. Phys.* **1971**, *54*, 3817.
22. Fehsenfeld F. C., Ferguson E. E.: *J. Geophys. Res., [Space Phys.]* **1969**, *74*, 5743.
23. Lineberger W. C., Puckett L. J.: *Phys. Rev.* **1969**, *187*, 286.
24. French M. A., Hills P. L., Kebarle P.: *Can. J. Chem.* **1973**, *51*, 456.
25. Brasseur G., Chatel A.: *Ann. Geophys.* **1983**, *1*, 173.
26. Nonella M., Huber J. R., Ha T.-K.: *J. Phys. Chem.* **1987**, *91*, 5203.
27. Uhlár M., Pitonak M., Černušák I.: *Mol. Phys.* **2005**, *103*, 2309.
28. Lee C., Yang W., Parr R. G.: *Phys. Rev. B* **1988**, *37*, 785.
29. Becke A. D.: *Phys. Rev. A* **1988**, *38*, 3098.
30. Bartlett R. J., Stanton J. F. in: *Reviews in Computational Chemistry* (K. B. Lipkowitz and D. B. Boyd, Eds), Vol. 5, p. 65. VCH Publishers, Inc., New York 1994.
31. Woon D. E., Dunning T. H., Jr.: *J. Chem. Phys.* **1994**, *100*, 2975.
32. Urban M., Noga J., Cole S. J., Bartlett R. J.: *J. Chem. Phys.* **1985**, *83*, 4041.

33. Bartlett R. J., Watts J. D., Kucharski S. A., Noga J.: *Chem. Phys. Lett.* **1990**, *165*, 513.
34. Boys S. F., Bernardi F.: *Mol. Phys.* **1970**, *19*, 553.
35. Frisch M. J., Trucks G. W., Schlegel H. B., Scuseria G. E., Robb M. A., Cheeseman J. R., Montgomery J. A., Jr., Vreven T., Kudin K. N., Burant J. C., Millam J. M., Iyengar S. S., Tomasi J., Barone V., Mennucci B., Cossi M., Scalmani G., Rega N., Petersson G. A., Nakatsuji H., Hada M., Ehara M., Toyota K., Fukuda R., Hasegawa J., Ishida M., Nakajima T., Honda Y., Kitao O., Nakai H., Klene M., Li X., Knox J. E., Hratchian H. P., Cross J. B., Bakken V., Adamo C., Jaramillo J., Gomperts R., Stratmann R. E., Yazyev O., Austin A. J., Cammi R., Pomelli C., Ochterski J. W., Ayala P. Y., Morokuma K., Voth G. A., Salvador P., Dannenberg J. J., Zakrzewski V. G., Dapprich S., Daniels A. D., Strain M. C., Farkas O., Malick D. K., Rabuck A. D., Raghavachari K., Foresman J. B., Ortiz J. V., Cui Q., Baboul A. G., Clifford S., Cioslowski J., Stefanov B. B., Liu G., Liashenko A., Piskorz P., Komaromi I., Martin R. L., Fox D. J., Keith T., Al-Laham M. A., Peng C. Y., Nanayakkara A., Challacombe M., Gill P. M. W., Johnson B., Chen W., Wong M. W., Gonzalez C., Pople J. A.: *Gaussian 03*, revision B.04. Gaussian Inc., Pittsburg (PA) 2003.
36. Stanton J. F., Gauss J., Watts J. D., Nooijen M., Oliphant N., Perera S. A., Szalay P. G., Lauderdale W. J., Kucharski S. A., Gwaltney S. R., Beck S., Balkova A., Bernholdt D. E., Baeck K. K., Rozyczko P., Sekino H., Hober C., Bartlett R. J.: *ACES II* is a program product of the Quantum Theory Project, University of Florida. Integral packages included are VMOL (J. Almlöf and P. R. Taylor), VPROPS (P. Taylor), ABACUS (T. Helgaker, H. J. Aa. Jensen, P. Jørgensen, J. Olsen and P. R. Taylor) 2005.
37. Schaftenaar G., Noordik J. H.: *J. Comput.-Aided Mol. Des.* **2000**, *14*, 123.